Published in final edited form as:
Magn Reson Med. 2009 June ; 61(6): 1533–1539. doi:10.1002/mrm.21921.

Non-Contrast-Enhanced Flow-Independent Peripheral MR Angiography with Balanced SSFP

Tolga Çukur[1], **Jin H. Lee**[1], **Neal K. Bangerter**[2], **Brian A. Hargreaves**[2], and **Dwight G. Nishimura**[1]

[1]Magnetic Resonance Systems Research Laboratory, Department of Electrical Engineering, Stanford University, Stanford, California

[2]Department of Radiology, Stanford University, Stanford, California

Abstract

Flow-independent angiography is a non-contrast-enhanced technique that can generate vessel contrast even with reduced blood flow in the lower extremities. A method is presented for producing these angiograms with magnetization-prepared balanced steady-state free precession (bSSFP). Because bSSFP yields bright fat signal, robust fat suppression is essential for detailed depiction of the vasculature. Therefore, several strategies have been investigated to improve the reliability of fat suppression within short scan times. Phase-sensitive (PS) SSFP can efficiently suppress fat; however, partial volume effects due to fat and water occupying the same voxel can lead to the loss of blood signal. In contrast, alternating repetition time (ATR) SSFP minimizes this loss; however, the level of suppression is compromised by field inhomogeneity. Finally, a new double-acquisition ATR-SSFP technique reduces this sensitivity to off-resonance. In vivo results indicate that the two ATR-based techniques provide more reliable contrast when partial volume effects are significant.

Keywords

peripheral angiography; non-contrast-enhanced; magnetic resonance angiography; SSFP; fat suppression

Introduction

Magnetic resonance angiography (MRA) of the extremities can help in the diagnosis of conditions such as peripheral vascular occlusion, peripheral arterial disease and Raynaud's disease. The main challenges for this application are the inherently slow blood flow and large volumetric coverage requirements in the lower extremities.

To date, there have been two main groups of MRA techniques for the extremities. Contrast-enhanced methods have been successfully used in the lower extremities (1–4); however, the bolus timing requirements limit the spatial resolution and signal-to-noise ratio (SNR). Furthermore, administration of gadolinium-based contrast agents introduces the risk of nephrogenic systemic fibrosis in patients with renal disease (5). Therefore, there has been renewed interest in non-contrast-enhanced MRA methods. Most of these techniques can effectively generate the desired blood-to-background contrast by relying on flow. However, the performance of flow-based techniques such as phase-contrast (6,7) or time-of-flight

Address correspondence to: Tolga Çukur, Packard Electrical Engineering, Room 210, 350 Serra Mall, Stanford, CA 94305-9510, TEL: (650) 725-7005, cukur@stanford.edu.

angiography (8,9) can be limited by reduced blood flow rate in the extremities, particularly with severe atherosclerotic disease. There are other flow-dependent techniques that can cope with slow flow more successfully such as fresh-blood imaging (FBI) (10,11). FBI subtracts diastolic- and systolic-triggered fast spin-echo acquisitions to produce high-resolution angiograms with reliable background suppression, but improper timing of the trigger delays can lead to blood signal loss in the subtraction images.

While most MRA techniques rely on contrast agents and/or flow to generate contrast, flow-independent angiography (FIA) (12,13) exploits differences in T1 and T2. This allows FIA to produce vessel contrast even in cases of slow flow. In early FIA work, magnetization-preparation schemes were combined with fast 3D imaging to generate contrast; however, the SNR efficiency was limited (13). Recently, FIA angiograms have been produced with magnetization-prepared balanced steady-state free precession (bSSFP) sequences (14,15) and centric phase-encode ordering to overcome this limitation (16).

Although bSSFP yields high SNR within short scan times, bright fat signal often obscures visualization of the underlying vasculature. In this study, we examined three different methods for reducing the fat signal in FIA angiograms: phase-sensitive (PS) SSFP (17), alternating repetition time (ATR) SSFP (18), and a new double-acquisition ATR-SSFP method (19). PS-SSFP is fast and efficient, but partial volume averaging can cause loss of blood signal in the vicinity of bone marrow and subcutaneous fat tissue. ATR-SSFP can instead be used to create a stop-band around the fat resonance (18) and reduce partial volume artifacts with little increase in scan time. However, the level of suppression is more sensitive to field inhomogeneity than PS-SSFP. In these cases, a new double-acquisition ATR-SSFP method can be employed to improve the stop-band at the expense of lengthened scan time (19).

We can produce FIA angiograms of the extremities with detailed depiction of the vasculature within several minutes, without the need for an intravenous contrast agent. The desired vessel contrast is generated by coupling magnetization-prepared three-dimensional Fourier transform (3DFT) bSSFP acquisitions with adequate fat suppression techniques. In cases where partial volume effects are not dominant (e.g., resolution $< 0.7\ mm^3$ in the extremities), PS-SSFP might be preferred to decrease the sensitivity to field inhomogeneity. However, ATR-based techniques generate more reliable contrast in the presence of considerable partial voluming.

Methods

Pulse Sequence Overview

A magnetization-prepared 3D bSSFP sequence with segmented k-space acquisition is used to produce FIA angiograms. The sequence starts with a magnetization-preparation module that has optional inversion-recovery and T2-preparation sections. When necessary, a nonselective inversion pulse is applied to reduce the signal from long-T1 fluids such as synovial fluid or edema. For improving the T2-dependent (blood-muscle, arterial-venous) contrast, a segmented adiabatic B1-insensitive rotation (BIR-4) pulse was used for T2-Preparation (20). The BIR-4 pulse offers immunity to main field and radio-frequency (RF) excitation field inhomogeneities. A diagram of the sequence showing all the available modules is displayed in Fig. 1.

A limited number of phase encodes can be acquired with the desired contrast due to the transient nature of magnetization preparation. To capture this contrast effectively, centric phase-encode ordering (a square spiral for 3DFT (21)) is employed and k-space is segmented into several interleaves (16). After a certain number of phase encodes are acquired, the magnetization is allowed to recover to equilibrium and preparation is repeated prior to the acquisition of the next interleaf. A linear ramp catalyzation is used, following magnetization preparation, to dampen transient signal oscillations (22).

Because frequent repetition of the magnetization preparation reduces the scan efficiency, multiple phase encodes are acquired after a single preparation. This leads to a transient acquisition, where a mixture of prepared and steady-state contrast is captured. Figure 2 shows the transient bSSFP signal simulated for different preparation schemes: no preparation, only inversion recovery, only T2-preparation, and both inversion recovery and T2-preparation. The following approximate relaxation parameters were chosen from literature (13,23–25): T1/T2 = 1000/220 ms for arterial blood, 1000/120 ms for venous blood (assuming 70-percent oxygen saturation in peripheral venous blood (26)), 870/50 ms for muscle and 4000/2000 ms for synovial fluid. The sequence parameters were: $\alpha = 60°$, TR/TE = 4.6/2.3 ms, TI (inversion time) = 2 s, T2-preparation time = 80 ms, and a 10-excitation linear ramp catalyzation. The flip angle and T2-preparation time were chosen to optimize the initial blood-muscle contrast while maintaining as low a specific absorption rate (SAR) as possible. The inversion time was adjusted to produce low signal from synovial fluid during a 4–5 s acquisition window.

Fat Suppression

PS-SSFP places fat and water resonance peaks in the centers of adjacent pass-bands, which have a π-radian phase difference. To achieve this placement at 1.5 T, a TR of about 4.6 ms is needed. PS-SSFP provides uniform fat suppression, but it can underestimate the water signal within a voxel containing a mixture of fat and water. These partial volume effects can be mitigated with sufficient spatial resolution. However, the resultant artifacts can be significant when the achievable spatial resolution is limited by SNR and scan time considerations. Due to the large volumetric coverage requirements, the resolution needs to be lowered to maintain an adequate SNR for lower leg and foot angiograms. Hence, partial volume artifacts with PS-SSFP reduce the quality of the angiograms.

On the other hand, fat-suppressing ATR-SSFP uses two consecutive repetition times (TR1 and TR2) to create a stop-band centered at the fat resonance (18). Because ATR-SSFP employs a different phase-cycling scheme than bSSFP, its response is equivalent to a frequency-shifted bSSFP response at on-resonance. This slightly reduces the tissue signal for higher T1/T2 ratios, and the magnitude of the signal change increases with T1/T2. Therefore, the ATR signal exhibits slightly more T2-dependent characteristics than the bSSFP signal both in the steady-state and throughout the progression from the initial prepared-state to the steady-state.

Arterial blood, venous blood, and muscle signals were simulated for the previously listed relaxation parameters assuming: $\alpha = 60°$, TR1/TR2/TE = 3.45/1.15/1.725 ms, T2-preparation time = 80 ms, and a 10-excitation linear ramp catalyzation. The ATR-SSFP sequence, with 0-90-180-270 phase-cycling, yields higher signal and improved T2-contrast at the start of the acquisition following T2-preparation. The initial arterial blood-muscle contrast is approximately 3.9 for ATR-SSFP, and 3.3 for bSSFP. This difference in signal behavior can lead to improved background suppression with ATR-SSFP. On the other hand, the arterial-venous contrast following T2-preparation is roughly 1.6 for both ATR-SSFP and bSSFP.

Since ATR-SSFP reduces the fat signal at the time of data acquisition, the corresponding partial volume effects are reduced. It is important to note that the level of suppression in the ATR stop-band is a function of off-resonance. At the edges of the stop-band where large field inhomogeneity is experienced, the signal reaches up to approximately 50% of the pass-band signal, yielding ineffective fat suppression. Methods with improved stop-bands are needed when the fat signal cannot be sufficiently reduced through the whole imaging volume. Although ATR-SSFP achieves adequate fat suppression in the lower leg, high field inhomogeneity is observed in regions such as the foot due to their irregular shape. In this case, an improved fat suppression method that relies on two ATR-SSFP acquisitions can be used instead (19).

In regular ATR-SSFP, the phase of the RF excitation prior to the TR2-interval is selected to place the central null of the stop-band at the fat-resonance (−220 Hz at 1.5 T). This selection divides the stop-band into two equal-width segments, where one segment is in-phase and the other is out-of-phase with the on-resonant water signal. By decreasing the RF phase, we can shift the central null toward higher frequencies and extend the width of the in-phase segment. Alternatively, the out-of-phase segment can be extended by increasing the RF phase.

Fat suppression can be achieved by summing two separate acquisitions where the whole stop-band is respectively in-phase and out-of-phase with the water signal (19). In one variation of this method, RF phases of 45° (0-45-180-225) and 135° (0-135-180-315) are used to create a stop-band as wide as the regular ATR-SSFP stop-band, assuming TR1/TR2 = 3. Because the magnitude profiles of the two acquisitions are very similar around the fat-resonance, the resulting stop-band suppression is significantly improved. In another variation, RF phases of 45° and −45° are used to generate in-phase and out-of-phase acquisitions for all frequencies in the spectrum except for the ones within the pass-band. This choice of RF phases increases the width of the stop-band three times (for TR1/TR2 = 3).

Figure 3 compares the simulated magnetization profiles for the aforementioned fat suppression methods. The following parameters were assumed: $\alpha = 60°$, TR/TE = 4.6/2.3 ms (bSSFP) and TR1/TR2/TE = 3.45/1.15/1.725 ms (ATR-SSFP and the double-acquisition fat suppression method), and T1/T2 = 260/80 ms for fat (25). PS-SSFP uses the bSSFP profile, which has high pass-band signal at the fat resonance (−220 Hz at 1.5 T). ATR-SSFP reduces this signal by creating a stop-band; however, the amount of suppression is limited with field inhomogeneity. The ATR-based double-acquisition method can yield substantially reduced remnant signal in the stop-band. Alternatively, the stop-band can be widened to further improve immunity to field inhomogeneity at the expense of a lower level of suppression and approximately 11 percent reduction in the pass-band signal.

Imaging Parameters

Lower leg and foot angiograms were produced with the 3DFT bSSFP FIA sequence using a single-channel transmit-receive linear extremity coil (26 cm in length, 18 cm in diameter). The experiments were performed on a 1.5 T GE Signa Excite scanner with CV/i gradients. Fat signal was suppressed with PS-SSFP, ATR-SSFP, and the double-acquisition ATR method. The acquisition parameters were: $\alpha = 60°$, TR/TE = 4.6/2.3 ms for PS-SSFP, and TR1/TR2/TE = 3.45/1.15/1.7 ms for ATR-SSFP, 1 mm isotropic resolution, 25.6 cm × 12.8 cm × 12.8 cm FOV, ± 125 kHz bandwidth, 256 × 128 × 128 encoding matrix, T2-preparation time = 80 ms, a 10-excitation catalyzation, 4 interleaves, 19 s data acquisition window for each interleave, and a 4 s recovery time. The acquisition time for a single dataset was 1 min 28 s. The irregular shape of the foot led to high field inhomogeneity. Therefore, the double-acquisition method was modified to widen the stop-band as previously mentioned. All datasets were zero-padded to twice the initial matrix size prior to a maximum-intensity projection (MIP) to improve visualization of the vasculature.

This study was approved by our institutional review board. Four volunteers were scanned to produce FIA angiograms of the lower leg and the foot. Written, informed consent was obtained from all subjects. To quantitatively compare the level of background suppression and the reliability of vessel contrast, the arterial/venous and arterial blood/muscle contrast as well as scan-time-normalized contrast-to-noise-ratio (CNR) were measured. In the lower leg, measurements were performed in the popliteal, peroneal, and posterior tibial arteries. The arterial blood/muscle CNR was computed with the mean arterial signal. In the foot, the lateral plantar artery and dorsal metatarsal arteries were used to measure the arterial blood/muscle CNR. Homogeneous regions of arterial as well as neighboring venous and muscle signal were selected on the source images for the measurements. The noise was then estimated by

computing the standard deviation in the muscle region. The same tissue regions were used when comparing different techniques. The measurements from all subjects were averaged.

Results

Representative PS-SSFP, ATR-SSFP, and double-acquisition ATR angiograms of the lower leg are displayed in Fig. 4. The techniques mainly differ in their sensitivity to field inhomogeneity and partial volume effects. PS-SSFP uniformly removes the fat signal (Fig. 4.a), whereas the level of suppression degrades in regions of high field inhomogeneity with ATR-SSFP (Fig. 4.b). The double-acquisition ATR method improves the fat suppression in these regions (Fig. 4.c).

Partial volume cancellation creates stripe-like artifacts on vessels in the vicinity of fat tissue in the PS-SSFP image. On the other hand, ATR-based methods are more robust against these artifacts and dramatically improve the visualization of small vessels. Furthermore, the blood-muscle contrast is higher as a result of the increased blood-muscle signal difference following magnetization preparation for ATR-SSFP compared with bSSFP.

ATR-SSFP is a very effective direct fat suppression method; however, the width of its stop-band may be insufficient in the presence of high field inhomogeneity. ATR-SSFP usually yields significant remnant fat signal in the foot angiograms. For this case, the double-acquisition ATR method -tailored to increase the stop-band width- offers improved performance. MIPs of typical PS-SSFP, ATR-SSFP, and double-acquisition foot angiograms are shown in Fig. 5.

PS-SSFP again suffers from partial volume artifacts deteriorating the depiction of vasculature (Fig. 5.a). ATR-SSFP improves the depiction in regions of robust fat suppression; however, the residual fat signal reduces the visibility of the vessels in the remaining regions (Fig. 5.b). Finally, the double-acquisition method sufficiently reduces the fat signal in these regions, and suffers less from partial volume artifacts compared with PS-SSFP (Fig. 5.c). The improved fat suppression of the double-acquisition method yields superior depiction of the vasculature.

Table 1 lists the arterial/venous and arterial blood/muscle CNR (scan-time-normalized) and contrast measurements in the lower leg and foot angiograms. PS-SSFP and the double-acquisition ATR method have similar SNR efficiencies, while that of ATR-SSFP is approximately 22-percent higher due to its initially higher transient blood signal. Furthermore, the ATR-based techniques demonstrate 14-percent higher arterial blood/muscle contrast than bSSFP on average, which closely matches with the theoretical estimate of 17 percent. In turn, higher CNR values are achieved with ATR-based methods. Meanwhile, similar arterial/venous contrast values are observed for all three techniques, as predicted by theory.

Discussion

Flow-independent angiography (FIA) with magnetization-prepared bSSFP exploits the intrinsic MR properties to suppress the background signal. Therefore, it can yield high, isotropic spatial resolution even in cases of slow and non-pulsatile flow. Because reliable fat suppression is crucial for this application, we have investigated three methods with relatively short acquisition times: PS-SSFP, ATR-SSFP, and a double-acquisition ATR method.

There are several criteria for comparing the performance of these techniques: partial volume effects, sensitivity to field inhomogeneity, minimum scan time, and reconstruction complexity. In terms of partial volume effects, ATR-based techniques perform better and reduce small vessel loss compared to PS-SSFP. In terms of immunity to off-resonance, PS-SSFP and the double-acquisition method outperform ATR-SSFP. In regards to scan time, the double acquisition method requires twice the image acquisition time compared to PS- and ATR-SSFP.

Image registration might be needed with considerable patient motion between the two acquisitions. Finally, PS-SSFP requires the most complicated reconstruction including a region-growing phase-correction algorithm (17).

The investigated techniques can be extended to acquire larger FOVs and image at higher field strengths (3 T). The FOV was limited to 26 cm due to the size of the extremity coil used in this work. In fact, a FOV of 38 cm can be acquired in the readout (superior-inferior) direction without introducing severe artifacts assuming the current parameter values of 4.6 ms TR and 1 mm resolution. In our experience, banding artifacts become more severe if the FOV is extended in the other two dimensions. To mitigate these artifacts without reducing the TR, dual-acquisition phase-cycling (27) can be used for PS-SSFP, whereas partial-dephasing in the slice direction is compatible with ATR-based techniques (28).

Similar to large-FOV imaging, banding artifacts experienced at higher field strengths can be reduced with the aforementioned strategies. For fat suppression at 3 T, PS-SSFP requires an optimal TR of 2.3 ms (17), while the TR can be kept the same with ATR-based techniques (18,19). Although ATR deposits higher RF power at 1.5 T, the reduced TR of PS-SSFP at 3 T yields equivalent SAR values for both methods. The flip angles must be reduced to an approximate maximum of 50° at 3 T to comply with the SAR limits. Although this yields reduced blood/muscle contrast, the improved venous suppression at higher field strengths will be more beneficial (29).

Several other fat suppression methods for bSSFP reduce the fat signal without introducing significant partial volume artifacts. An efficient method is to apply spectrally-selective RF saturation pulses during the steady-state acquisitions (30); however, RF inhomogeneities and transient signal oscillations lead to artifacts. These problems can be avoided with linear-combination SSFP (31). This method effectively suppresses the fat signal, but places more demanding limitations on the TR selection than PS-SSFP or ATR-SSFP. A very simple double-acquisition method comprising a summation of in-phase and out-of-phase images has been proposed by Huang et al. (32,33). Although this method gives flexibility in the choice of TR, its stop-band width is limited.

Intriguing alternatives for fat suppression that are also robust to main-field inhomogeneity are multi-echo DIXON techniques (34,35). In order to be able to acquire three echoes within a single TR for the peripheral angiography applications, the TR has to be increased. Two phase-cycled datasets may need to be acquired to remove the resultant banding artifacts. Hence, the total scan time can be longer compared with the double-acquisition ATR fat suppression method used in this work, increasing the susceptibility to motion artifacts. Furthermore, the multi-echo techniques require a complicated reconstruction as opposed to the simple pixel-wise summation of the datasets in the double-acquisition ATR method.

Conclusion

Magnetization-prepared 3D bSSFP sequences can be coupled with fast fat suppression techniques to acquire flow-independent angiograms over 26 cm of the extremities in less than 3 minutes and without the need for contrast agents. If partial volume effects are mitigated by sufficiently high resolution, PS-SSFP may be preferred. However, ATR-based techniques generate improved vessel contrast in the lower extremities, where the limitations on the achievable resolution can lead to significant partial volume averaging. When necessary, a modified double-acquisition method can provide increased immunity against field inhomogeneity for ATR-SSFP.

Acknowledgments

This work was supported by National Institutes of Health (NIH) under Grant R01 HL039297, Grant R01 HL075803 and by GE Healthcare. The work of Tolga Çukur was supported by a Rambus Corporation Stanford Graduate Fellowship.

References

1. Creasy JL, Price RR, Prsbrey T, Goins D, Partain CL, Kessler RM. Gadolinium-enhanced MR angiography. Radiology 1990;175:280–283. [PubMed: 2315497]
2. Shetty AN, Shirkhoda A, Bis KG, Alcantara A. Contrast-enhanced three-dimensional MR angiography in a single breath-hold: a novel technique. AJR Am J Roentgenol 1995;165:1290–1292. [PubMed: 7572521]
3. Runge VM, Kirsch JE, Lee C. Contrast-enhanced MR angiography. J Magn Reson Imaging 1993;3:233–239. [PubMed: 8428091]
4. Prince MR. Body MR angiography with gadolinium contrast agents. Magn Reson Imaging Clin N Am 1996;4:11–24. [PubMed: 8673710]
5. Marckmann P, Skov L, Rossen K, Dupont A, Damholt MB, Heaf JG, Thomsen HS. Nephrogenic systemic fibrosis: suspected causative role of gadodiamide used for contrast-enhanced magnetic resonance imaging. J Am Soc Nephrol 2006;17:2359–2362. [PubMed: 16885403]
6. Axel L, Morton D. MR flow imaging by velocity-compensated/uncompensated difference images. J Comput Assist Tomogr 1987;11:31–34. [PubMed: 3805425]
7. Dumoulin CL, Souza PS, Walker MF, Wagle W. Three-dimensional phase contrast angiography. Magn Reson Med 1989;9:139–149. [PubMed: 2709992]
8. Marchal G, Bosmans H, Fraeyehoven LV, Wilms G, Hecke PV, Plets C, Baert AL. Intracranial vascular lesions: optimization and clinical evaluation of three-dimensional time-of-flight MR angiography. J Am Soc Nephrol 1990;175:443–448.
9. Nishimura DG. Time-of-flight MR angiography. Magn Reson Med 1990;14:194–201. [PubMed: 2345502]
10. Miyazaki M, Sugiura S, Tateishi F, Wada H, Kassai Y, Abe H. Non-contrast-enhanced MR angiography using 3D ECG-synchronized half-Fourier fast spin echo. J Magn Reson Imaging 2000;12:776–783. [PubMed: 11050650]
11. Miyazaki M, Takai H, Sugiura S, Wada H, Kuwahara R, Urata J. Peripheral MR angiography: Separation of arteries from veins with flow-spoiled gradient pulses in electrocardiography-triggered three-dimensional half-Fourier fast spin-echo imaging. Radiology 2003;227:890–896. [PubMed: 12702824]
12. Wright GA, Nishimura DG, Macovski A. Flow-independent magnetic resonance projection angiography. Magn Reson Med 1991;17:126–140. [PubMed: 2067389]
13. Brittain JH, Olcott EW, Szuba A, Gold GE, Wright GA, Irarrazaval P, Nishimura DG. Three-dimensional flow-independent peripheral angiography. Magn Reson Med 1997;38:343–354. [PubMed: 9339435]
14. Carr HY. Steady-state free precession in nuclear magnetic resonance. Phys Rev 1958;112:1693–1701.
15. Oppelt A, Graumann R, Barfuss H, Fischer H, Hartl W, Shajor W. FISP – a new fast MRI sequence. Electromedica 1986;54:15–18.
16. Bangerter, NK.; Hargreaves, BA.; Brittain, JH.; Hu, B.; Vasanawala, SS.; Nishimura, DG. 3D fluid-suppressed T2-prep flow-independent angiography using balanced SSFP. Proceedings of the 12th Annual Meeting of ISMRM; Kyoto. 2004. p. 11
17. Hargreaves BA, Vasanawala SS, Nayak KS, Hu BS, Nishimura DG. Fat-suppressed steady-state free precession imaging using phase detection. Magn Reson Med 2003;50:210–213. [PubMed: 12815698]
18. Leupold J, Hennig J, Scheffler K. Alternating repetition time balanced steady state free precession. Magn Reson Med 2006;55:557–565. [PubMed: 16447171]
19. Çukur T, Nishimura DG. Fat-water separation with alternating repetition time balanced ssfp. Magn Reson Med 2008;58:1216–1223.

20. Nezafat, R.; Derbyshire, JA.; Ouwerkerk, R.; Stuber, M.; McVeigh, ER. Spectrally selective B1 insensitive T2 preparation sequence for 3T imaging. Proceedings of the 14th Annual Meeting of ISMRM; Seattle. 2006. p. 596
21. Korin HW, Riederer SJ, Bampton AEH, Ehman RL. Altered phase encoding order for reduced sensitivity to motion corruption in 3DFT MR imaging. J Magn Reson Imaging 1992;2:687–693. [PubMed: 1446113]
22. Nishimura, DG.; Vasanawala, SS. Analysis and reduction of the transient response in SSFP imaging. Proceedings of the 8th Annual Meeting of ISMRM; Denver. 2000. p. 301
23. Wright GA, Hu BS, Macovski A. 1991 I.I. Rabi Award. estimating oxygen saturation of blood in vivo with MR imaging at 1.5 T. J Magn Reson Imaging 1991;1:275–283. [PubMed: 1802140]
24. Gronas R, Kalman PG, Kucey DS, Wright GA. Flow-independent angiography for peripheral vascular disease: Initial in-vivo results. J Magn Reson Imaging 1997;7:637–643. [PubMed: 9243381]
25. Bernstein, MA.; King, KF.; Zhou, XJ. Handbook of MRI pulse sequences. Vol. 1st ed.. Burlington, MA: Elsevier Academic Press; 2004.
26. Lee, T.; Stainsby, JA.; Hong, J.; Han, E.; Brittain, J.; Wright, GA. Blood relaxation properties at 3T – effects of blood oxygen saturation. Proceedings of the 11th Annual Meeting of ISMRM; Toronto. 2003. p. 131
27. Hargreaves BA, Bangerter NK, Vasanawala SS, Shimakawa A, Brittain JH, Nishimura DG. Dual-acquisition phase-sensitive SSFP water-fat separation. Magn Reson Imaging 2006;24:113–122. [PubMed: 16455400]
28. Hargreaves, BA. Partially dephased SSFP for elimination of dark bands. Proceedings of the 16th Annual Meeting of ISMRM; Toronto. 2008. p. 1357
29. Dharmakumar R, Hong J, Brittain JH, Plewes DP, Wright GA. Oxygen-sensitive contrast in blood for steady-state free precession imaging. Magn Reson Med 2005;53:574–583. [PubMed: 15723410]
30. Scheffler K, Heid O, Hennig J. Magnetization preparation during the steady-state: Fat-saturated 3D true FISP. Magn Reson Med 2001;45:1075–1080. [PubMed: 11378886]
31. Vasanawala SS, Pauly JM, Nishimura DG. Linear combination steady-state free precession MRI. Magn Reson Med 2000;43:82–90. [PubMed: 10642734]
32. Huang TY, Chung HW, Wang FN, Ko CW, Chen CY. Fat and water separation in balanced steady-state free precession using the Dixon method. Magn Reson Med 2004;51:243–247. [PubMed: 14755647]
33. Stafford RB, Sabati M, Mahallati H, Frayne R. 3D non-contrast-enhanced MR angiography with balanced steady-state free precession Dixon method. Magn Reson Med 2008;59:430–433. [PubMed: 18183607]
34. Reeder SB, Pineda AR, Wen Z, Shimakawa A, Yu H, Brittain JH, Gold GE, Beaulieu CH, Pelc NJ. Iterative decomposition of water and fat with echo asymmetry and least-squares estimation (IDEAL): application with fast spin-echo imaging. Magn Reson Med 2005;54:636–644. [PubMed: 16092103]
35. Hernando D, Haldar JP, Sutton BP, Ma J, Kellman P, Liang ZP. Joint estimation of water/fat images and field inhomogeneity map. Magn Reson Med 2008;59:571–580. [PubMed: 18306409]

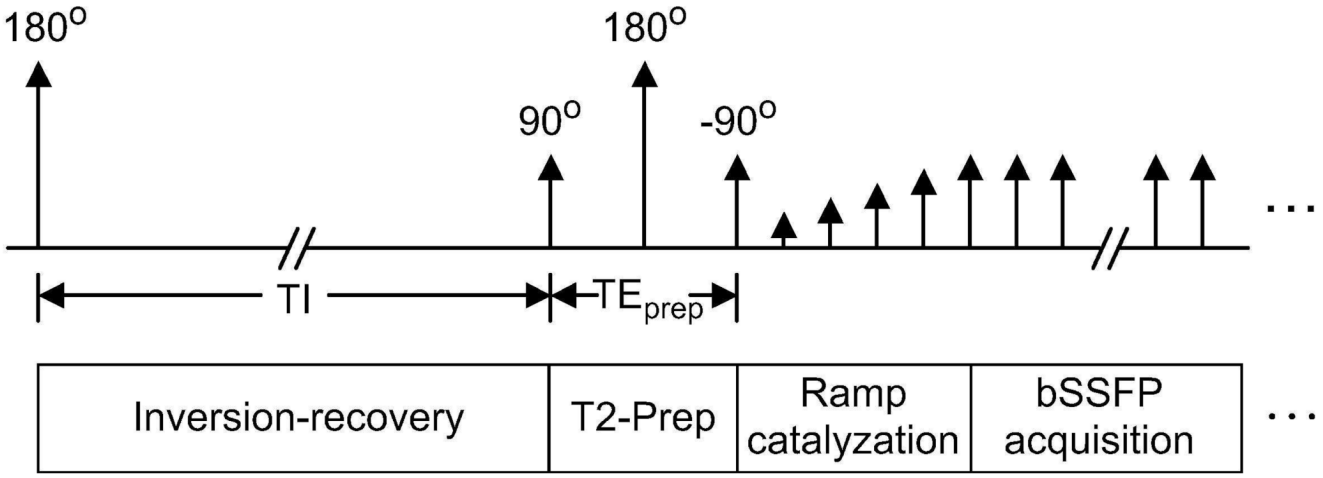

Figure 1.
Pulse sequence diagram. Optional inversion-recovery and T2-Preparation sections form the magnetization-preparation module. The bSSFP acquisition starts immediately following a ramped series of RF excitations.

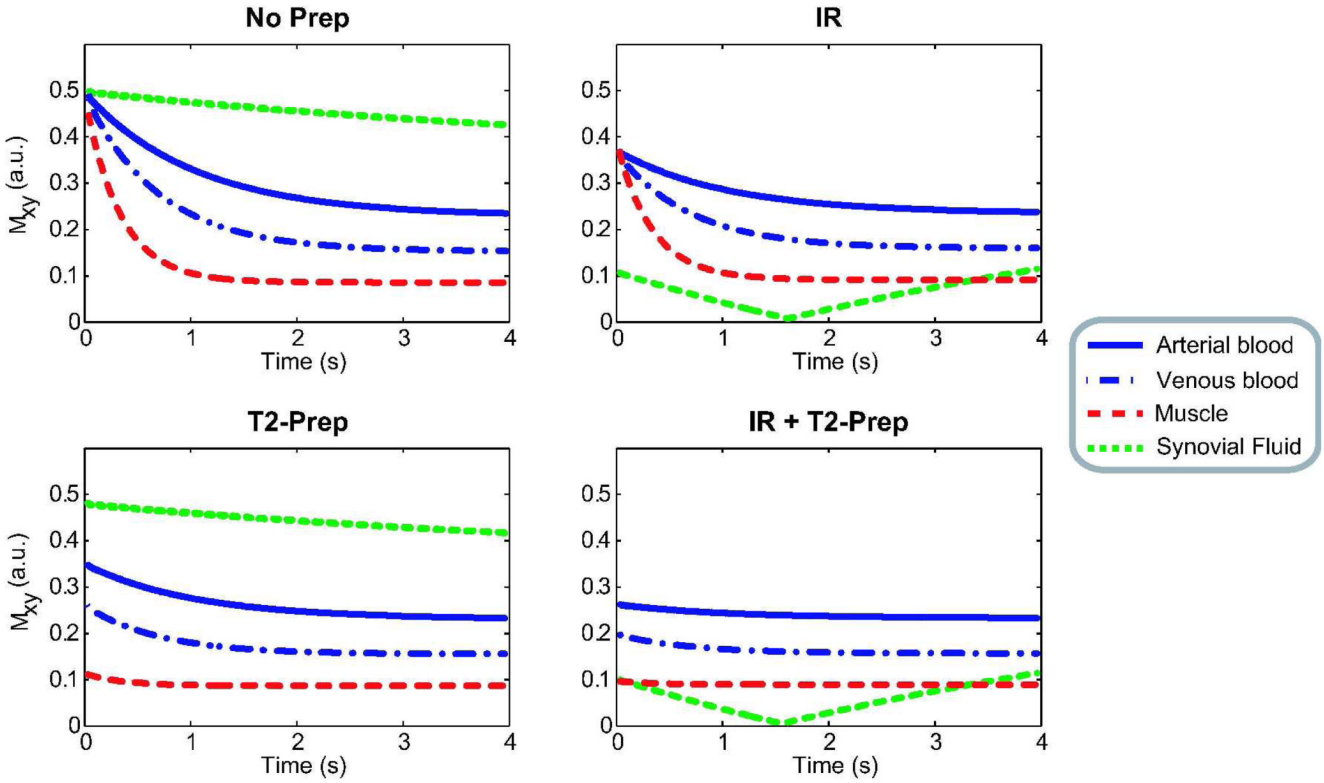

Figure 2.
The transient bSSFP signal is shown immediately after various types of magnetization preparation. The inversion-recovery sequence reduces the synovial-fluid signal for a finite time window at the expense of reduced signal. T2-preparation improves the initial blood-muscle and arterial-venous contrasts.

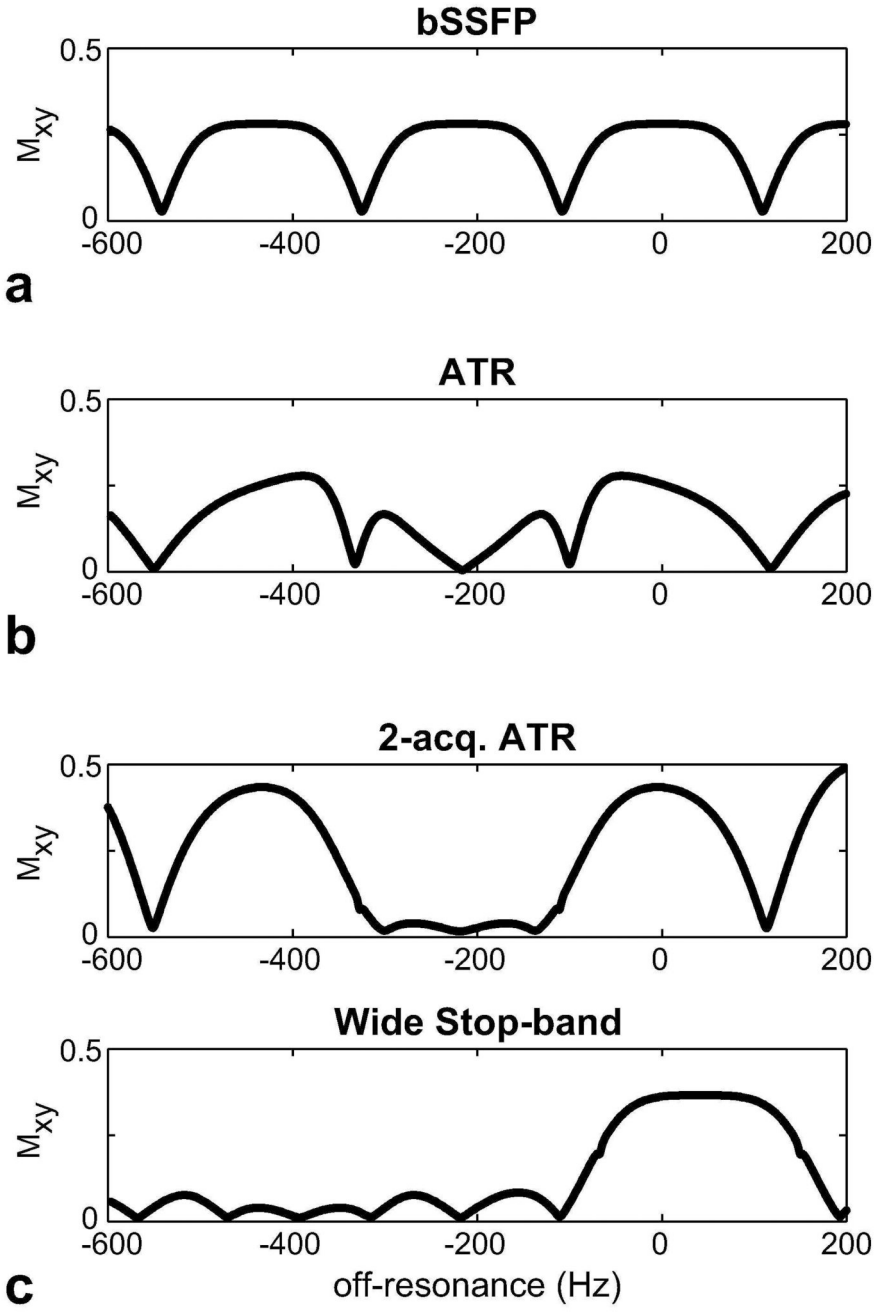

Figure 3.

The transverse magnetization profiles were simulated for **a:** bSSFP, **b:** ATR-SSFP sequences, and **c:** the ATR-based double-acquisition fat suppression method. ATR-SSFP creates a stop-band around the fat resonance; however, the residual stop-band signal with increasing field inhomogeneity limits the level of achievable suppression. On the other hand, the double-acquisition method robustly suppresses the fat signal. Furthermore, this method can be modified to widen the stop-band and provide increased immunity to field inhomogeneity.

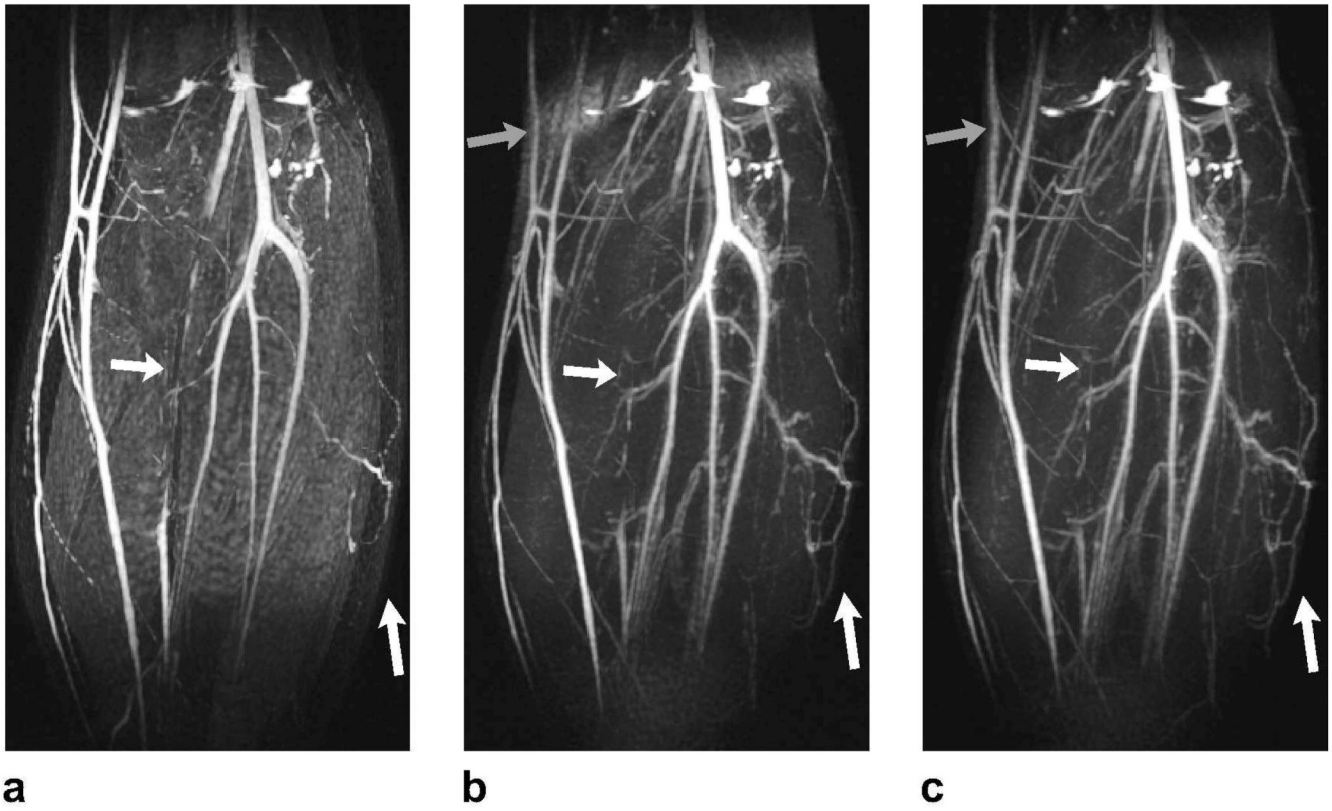

Figure 4.
Lower leg angiograms were produced with **a:** PS-SSFP, **b:** ATR-SSFP, and **c:** the double-acquisition ATR fat suppression method. The white arrows point to regions of vessel signal loss due to partial volume effects with PS-SSFP. In contrast, ATR-based methods reduce these artifacts and significantly improve small vessel visualization. It is important to note that higher blood-muscle contrast is observed in the ATR angiograms. The gray arrows point to the regions where field inhomogeneity limits the level of fat suppression in the ATR-SSFP angiogram, whereas the double-acquisition method reliably reduces the fat signal.

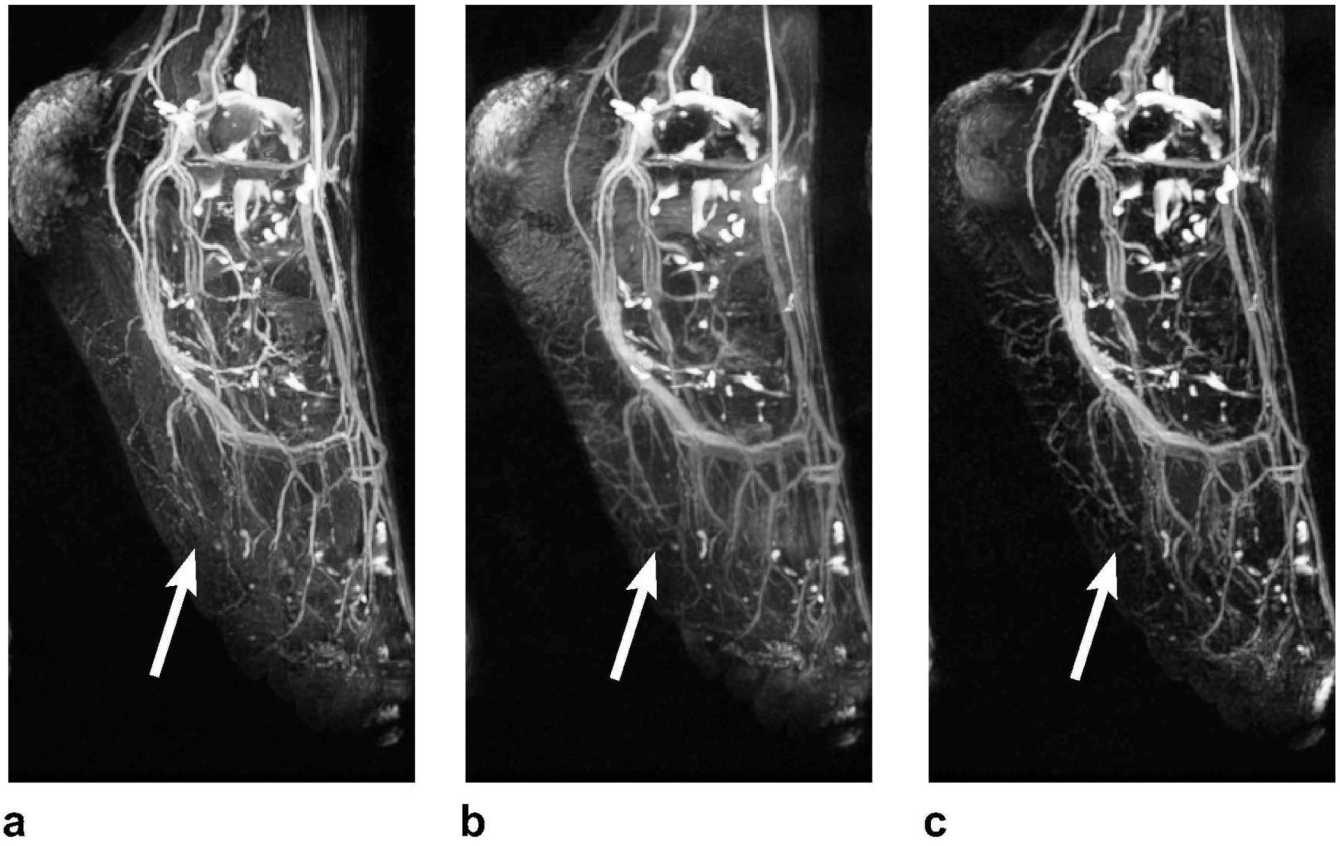

Figure 5.
Foot angiograms acquired with **a:** PS-SSFP, **b:** ATR-SSFP, and **c:** the double-acquisition ATR fat suppression. PS-SSFP achieves uniform suppression, but suffers from partial volume artifacts. On the other hand, ATR-SSFP reduces the fat signal to varying levels, deteriorating the visualization of underlying vessels toward the ankle. Finally, the double-acquisition method achieves a level of suppression adequate for clearly depicting the vasculature. The arrows point to the regions where partial volume artifacts lead to loss of blood signal with PS-SSFP. In these regions, the blood-background contrast is higher with ATR-SSFP compared to PS-SSFP.

Table 1

The arterial/venous (A/V) and arterial blood/muscle (A/M) CNR (scan-time-normalized) and contrast were measured in PS-SSFP, ATR-SSFP, and the double-acquisition ATR angiograms. In the lower leg, the first set of arterial/venous measurements were performed in the popliteal artery itself, whereas the second set was collected in peroneal and posterior tibial branches. In the foot, the first and second sets of measurements were performed in the lateral plantar artery and dorsal metatarsal arteries respectively.

Method	PS-SSFP	ATR-SSFP	Double Acq.
A/V 1: CNR	14.48	20.80	16.22
(Calf) Contrast	2.01	2.07	2.04
A/V 2: CNR	8.98	11.12	8.92
(Calf) Contrast	1.68	1.64	1.62
A/M : CNR	16.13	22.91	18.81
(Calf) Contrast	2.73	3.01	3.16
A/M 1: CNR	11.31	15.65	16.00
(Foot) Contrast	2.63	2.76	3.29
A/M 2: CNR	7.16	9.42	9.47
(Foot) Contrast	2.03	2.06	2.36